

## PRINTING PARAMETER OPTIMIZATION OF EXTRUDED METAL PASTE BY RESPONSE SURFACE TECHNIQUE

Marshall Norris<sup>α</sup>, Ismail Fidan<sup>β</sup>

<sup>α</sup>Department of Mechanical Engineering, College of Engineering  
Tennessee Technological University, Cookeville, TN 38505

<sup>β</sup>Department of Manufacturing and Engineering Technology, College of Engineering  
Tennessee Technological University, Cookeville, TN 38505

### Abstract

This research is focused on optimizing printing parameters using the response surface (RS) methodology. When printing parameters are not optimized, the resulting prints contain an unacceptable surface finish, porosity, or the print fails entirely as the lower portion of the print will not be able to withstand the weight of consecutive layers. Printing parameters, layer height, and percent infill were adjusted for the study while material flow rate and print head speed were held constant. RS is a statistical based eigenvalue process that uses data points on a three-dimensional curve to predict and identify local maxima or minima. For this study, RS was used to identify the inflection point where surface finish is optimized. A starting point for the parameters begins with rheological characterization of the paste and geometric modeling (or brute force approach). Once the parameters are able to produce an acceptable surface finish, the RS approach was used to refine printing parameters.

Keywords: Additive Manufacturing, Metallic Paste, 17-4PH, Parameter Optimization, Response Surface

### Introduction

This research was focused on optimizing printing parameters of Material Extrusion (MEX) metallic paste using the RS methodology [1][2]. Today, MEX is one the seven additive manufacturing (AM) techniques, and it is popularly used in a high number of industrial practices [3][4]. The motivation for this optimization is that if the printing parameters are not optimized, the resulting prints will either contain unwanted porosity, an unacceptable surface finish, or incomplete print as the lower portion of the print must withstand the weight of each consecutive layer. Printing was performed via MEX on a XYZ Davinci 1.0 with a modified extruder adapted for extrusion of metallic paste comprised of 17-4PH and hydroxypropyl methylcellulose (HPMC), an organic binder expected to burn out completely leaving no residual material in the metallic matrix [5]. The paste was mixed homogeneously, then inserted into a hopper which was pressurized using unfiltered air at approximately 10 psi. In this modified design, the pressure controls the paste extrusion speed or in this case, the volumetric flowrate as the mixture was held constant. The nozzle diameter was designed at 0.015” (~0.4mm) and the traverse speed of the print head was held at a constant 5mm/s.

RS is a statistical based process that uses multiple data points of a curve and curve fitting to determine local maxima or minima [6]. As the primary fitness criteria, RS was used to identify

the inflection point in the printing parameters where surface roughness was optimized. As a secondary fitness criterion, density was also sudo-optimized. A local starting point for the parameters layer height and % infill begins with the rheological characterization of the paste. Once the parameters are deemed close, the RS approach was used to refine printing parameters.

Methylcellulose (MC) was selected as the binder as [7] proposed the eco-friendliness of printing ceramics as MC is a naturally occurring polymer and is effective in low concentrations. Other research such as [8] printed metal paste using polymerization of an organic monomer methacrylate-2-hydroxy ethyl and toluene, with 316L particles 62.5 % by volume; the ratio of this paste for this research was 99.7% 17-4PH and 0.3% MC. [9] printed 316L samples on an MEX machine with 55% 316L powder and the balance was two proprietary polymers. Test prints used for printing optimization included a box with a width of 25mm and wall thickness of 5mm while this research used solid ½” cubes. Thompsons printing focused on optimization of dimensions, surface finish, and density by adjusting fan speed, print bed temperature, nozzle temperature. [10] used ANOVA and printed Ultrafuse 316L to optimize isotropic shrinkage, material properties, and final density based on varying the parameters nozzle temperature, layer thickness, and flow rate. In this research, the flow rate was held constant, it was printed with an ambient nozzle temperature. Zhang et al. also predicted dimensional changes of sintered MEX components using a bronze infilled PLA material from Ultimet [11]. Zhang used linear regression, including interactions, and a machine learning (ML) algorithm to optimize his printing parameters. However, Zhang printed over a hundred samples to identify optimized parameters and one outcome of using the RS method is that it expedites the optimization process.

### **Methodology**

For this study, the paste was comprised of spherical 17-4PH with diameters between 15-45 $\mu$ m, MC, and fluidized with water. First the polymer was fluidized until uniform blended at room temperature, then the metallic powder was added into the mixture and printed using the modified printer. The geometry of interest was a cube due to the ease of measurement and was 0.5 inches on each side. The geometry was designed in SolidWorks and sliced using the Cura packaged within Repetier Host. Speeds were set in accordance with the work done by [12] to balance appropriate drying of each layer before the next was printed but such that the material in the nozzle does not dry out as can occur when printing small layers due to heat transfer through the deposited material. Infill density and layer height were adjusted per the Design of Experiment (DOE) [13]. The nozzle designed for paste extrusion is shown in Figure 1.

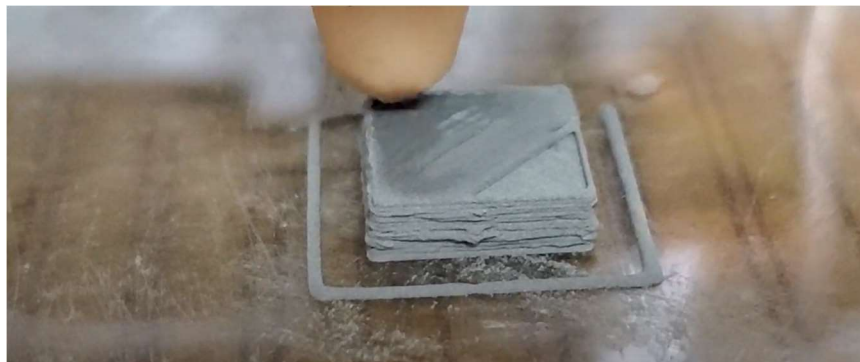


Figure 1: 0.015 inch paste printing nozzle

During printing, if the infill is not optimized, this will result in either excess material deposited leading to overfill and rougher surface finish, or a decrease in density and increase in porosity (see Figure 2A) in the final printed components. Additionally, when the layer height is not optimized, either consecutive layers will be too far from the previous layers and slump (see Figure 2B) or will again result in too much deposited material and increased surface roughness.

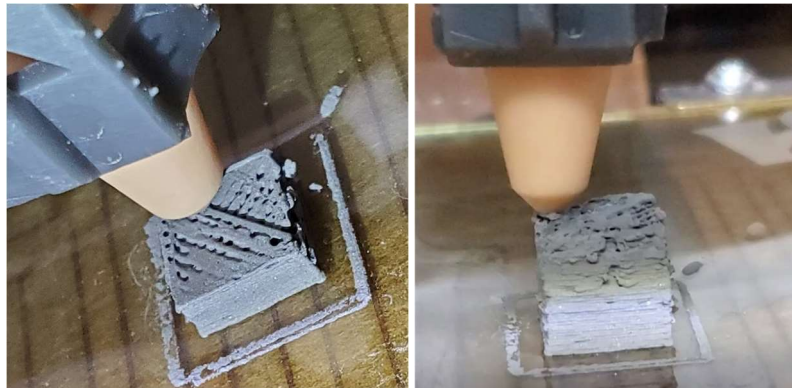


Figure 2: Un-optimized infill results in (A) voids in final print and (B) dysfunctional layers

While some research is focused on alternative optimization techniques such as Zhang et al.[11], using RS requires less test samples and results in better accuracy over the test domain than ML techniques such as Deep Learning or by hand as performed by [14]. For this test, the min and max for both variables were printed along with the average of the variables to create a first order surface (see Figure 3) in the infill vs layer-height space. Figure 4 provides an example of how the variables fit into a nonlinear space but was approximated initially to find the direction of the slope and provide guidance on what the next set of testing may include.

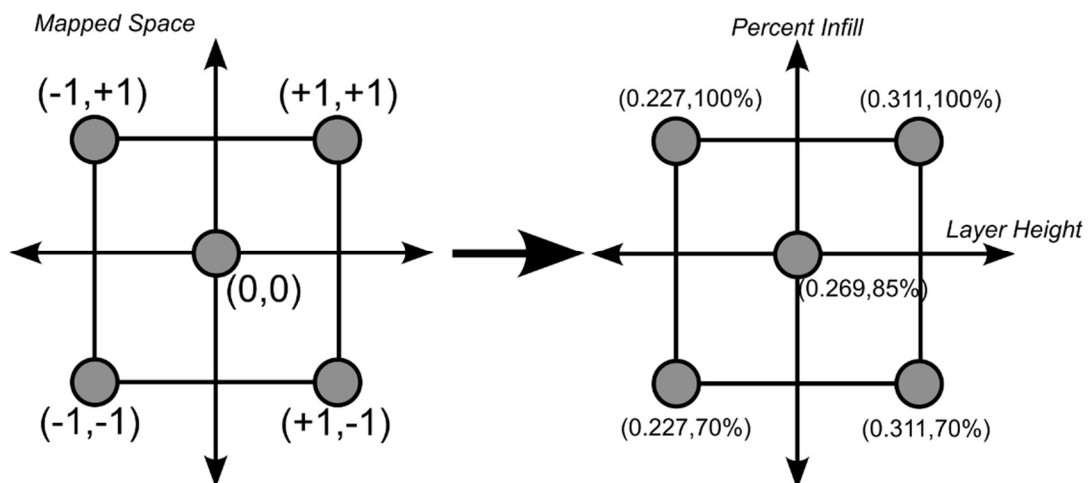


Figure 3: Five design points for infill and layer height variables in mapped space

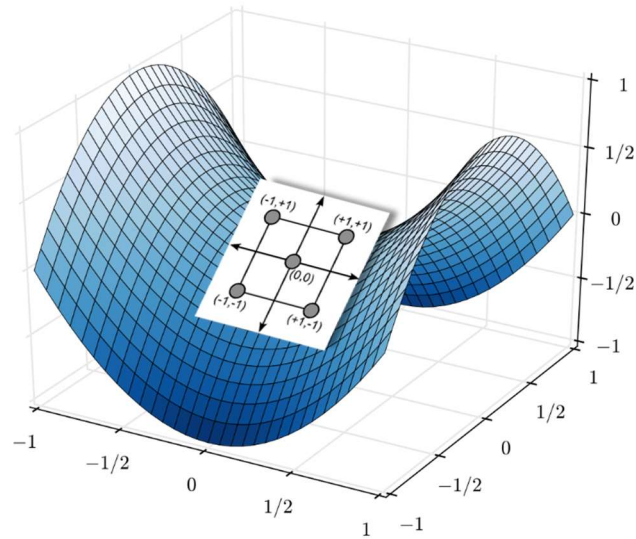


Figure 4: An example of a mapped linear surface onto a nonlinear surface

The generalized second dimensional linear regression model for this is

$$y_i = \beta_0 + \beta_1 x_{1i} + \beta_2 x_{2i} + \varepsilon_i \quad 1$$

In this research,  $y$  was surface roughness and  $x_1$  and  $x_2$  are variables shown below. Infill was varied between 70% to 100% with a mean of 85 and a span of 30. Layer height was adjusted between 0.227 to 0.311 inches with a mean of 0.269 and a span of .084. Parameters are then modeled as shown in coded parameters as  $\left(\frac{x_i - \text{Parameter average}}{\text{Parameter range}}\right)$ . The resulting equations for infill and layer height are calculated as

$$x_1 (\text{Infill}) = \left(\frac{x_1 - 85}{30}\right) \quad 2$$

$$x_2 (\text{Layer height}) = \left(\frac{x_2 - .269}{.084}\right) \quad 3$$

The results from this analysis shown in Figure 5 include Model Sum of Squares, an F and P value indicating fit of the model, a lack of fit value, an indication of how much error was included in the model, and a corrected total sum of squares. An  $R^2$  and adjusted  $R^2$  value is also provided to determine how well the data was represented by the model as well as an adjustment for how many predictors are used. Parameter estimates for the regression model are given in both mapped space and in variable space. The model suggests a low adherence to the model proposed. It is assumed that this is largely due to the temperature variation in the material within the nozzle as the temperature alters the viscosity. This could be verified by a Taguchi Study better controlling the temperatures inside the printing material [15].

Parameter Estimates					
Variable	DF	Parameter Estimate	Standard Error	t Value	Pr >  t
Intercept	1	0.51710	0.00899	57.55	0.0003
A	1	0.01750	0.01005	1.74	0.2236
B	1	0.01825	0.01005	1.82	0.2109

Figure 5: Output from the analysis for surface roughness in SAS

### Results

The results then return these values of  $\beta_0$ ,  $\beta_1$ , and  $\beta_2$ , the linear regression curve then takes the form

$$y_{sRoughness} = .517 + 0.0175 * x_1 + 0.01825 * x_2 \quad 4$$

and similarly for the regression for weight

$$y_{wei} = 8.53 + 0.655 * x_1 - 0.705 * x_2 \quad 5$$

At this point, there are several approaches to multiparameter optimization. [16] proposed that outputs should be ranked on terms of importance and near optimal settings can be used following a process of Classification And Regression Trees (CART). Alternatively, Singh et al. uses Matlab to minimize both functions as they are equally important [17] using a pareto front approach. In the case of this reasearch, the primary objective was to reduce the surface roughness as this is required to minimize post machining. A secondary objective was to reduce porosity and increase density to ensure useability of components and their strength. However, there are other post processing routines that are used to smooth cast components like sand blasting or, for internal features, abrasive flow.

Mapping, for example, the surface roughness response variables back to the test variable space results in the following equations:

$$\begin{pmatrix} 0.175 \\ 0.018 \end{pmatrix} = \begin{pmatrix} \left( \frac{x_1 - 85}{30} \right) \\ \left( \frac{x_2 - .269}{.084} \right) \end{pmatrix} \quad 6$$

$$\text{or } \begin{pmatrix} x_1 \\ x_2 \end{pmatrix} = \begin{pmatrix} 90.25\% \\ 0.270 \end{pmatrix} \quad 7$$

Since 90.25% infill and 0.270 layer height are within the test domain, a re-centering of the test parameters according to these new printing parameters was not necessary. Had the results fallen outside the test domain, new values for the independent variables would have been selected and the study performed a second time. Once the domain was determined new test pieces were

printed to identify the nonlinear curve on the layer-height vs infill domain as shown in Figure 6. In 2D space, 9 points are evaluated to capture curvature in the 3D space of interest.

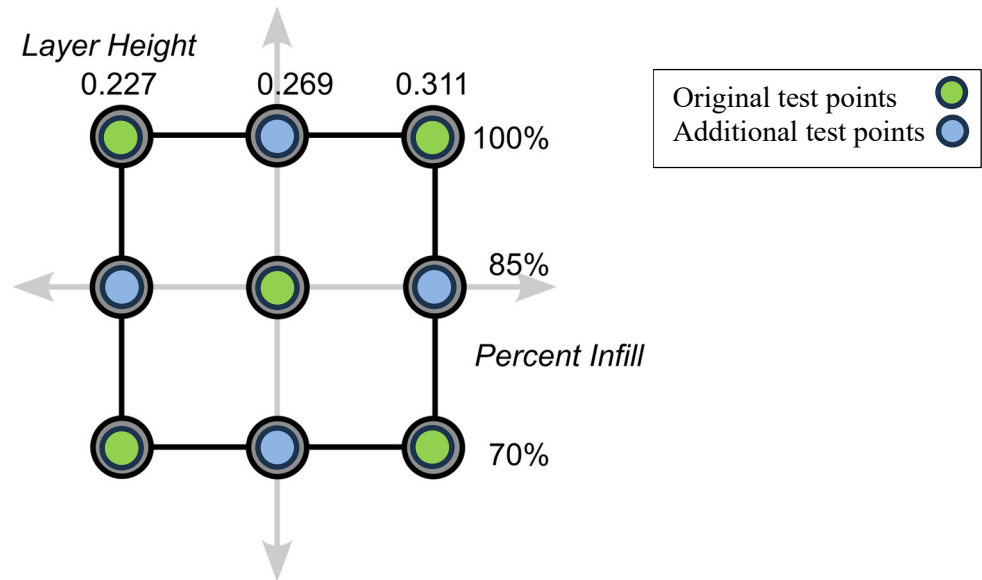


Figure 6: Additional prints provide nonlinear infill-vs-layer-height domain

The RS calculation then solved for eigenvalues and eigenvectors along with coded and uncoded values of the infill and Layer-height (see Figure 7). The inflection (optimized) point is shown as 0.5229 inches while the cube was originally modeled at 0.5. It is assumed the majority of the variance is attributed to temperature gradients within the printed material, which while the bed temperature was held constant, the thermal gradients will be different based on the infill structure. As the temperature of the material inside the nozzle increases, the paste becomes more viscous and introduces variability into the prints. This could be accounted for using a Taguchi Study where temperature flux was accounted for.

Factor	Critical Value	
	Coded	Uncoded
infill	0.381843	90.727651
LayerH	0.882080	0.294147
Predicted value at stationary point: 0.522928		

Figure 7: Optimized values for surface roughness

The measurement of fitness in this study was the density and surface roughness in a similar manner as [18] of the printed materials. Since the un-sintered printed materials are soft in nature, a standard profilometer could not be used for roughness measurements. A Keyence IM 8030T optical comparator was used instead to measure variation in surface and in this study the maximum variation in surface height Rz was used. The optimized results from the preliminary study are shown in Figure 8.



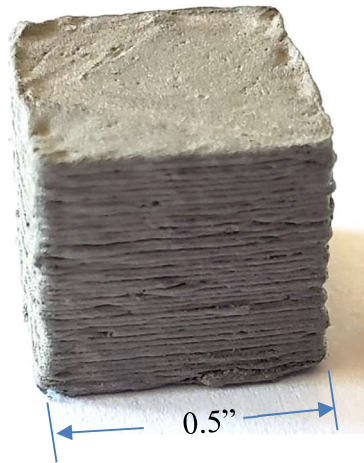


Figure 8: Final result using the grid fill pattern

In addition to minimizing surface roughness, a secondary objective was to maximize the density of the print by minimizing porosity similarly to [19] using RS instead of ML. The theoretical weight for the paste is 8.6g for a 0.5in cube. Measurements of the optimized printed cube show that the density is acceptable. Regression on weight provided a similar printing configuration with an infill of 90.49% and layer height of 0.229mm, a variation of 0.2% on infill and 29% on layer height. The predicted optimal weight shown in Figure 9 is 8.8g which is a departure from the theoretical weight by 2%. Depending on the weighted significance of final density versus surface roughness, the difference could be split proportionally by weighting.

Factor	Critical Value	
	Coded	Uncoded
infill	0.366150	90.492249
LayerH	-0.657074	0.229700
Predicted value at stationary point: 8.808172		

Figure 9: Optimal printing parameters for weight

### Conclusions

This research study focuses on optimizing the printing parameters of MEX cubes printed with metallic paste using the RS methodology. The primary motivation for this optimization is to address issues such as porosity, surface finish, and incomplete prints that may occur if the parameters are not optimized. Printing is performed using a modified extruder on a XYZ Davinci 1.0 printer, with the metallic paste consisting of 17-4PH spherical powder and HPMC as a binder. The RS methodology is employed to identify the inflection point in the printing parameters where surface roughness is optimized, with density also being considered as a secondary criterion. This research involves modeling and regression analysis to understand the relationship between these parameters and surface roughness and density. The findings of the overall study contain a number of contributions to the AM knowledge base, and the current results are favorable for professionals involved in managing MEX processes.

## References

- [1] A. Gupta *et al.*, “Material extrusion of thermoplastic acrylic for intraoral devices: Technical feasibility and evaluation,” *J Mech Behav Biomed Mater*, vol. 143, p. 105950, Jul. 2023, doi: 10.1016/J.JMBBM.2023.105950.
- [2] A. I. Khuri and S. Mukhopadhyay, “Response surface methodology,” *Wiley Interdiscip Rev Comput Stat*, vol. 2, no. 2, pp. 128–149, Mar. 2010, doi: 10.1002/WICS.73.
- [3] O. Huseynov, S. Hasanov, and I. Fidan, “Influence of the matrix material on the thermal properties of the short carbon fiber reinforced polymer composites manufactured by material extrusion,” *J Manuf Process*, vol. 92, pp. 521–533, Apr. 2023, doi: 10.1016/J.JMAPRO.2023.02.055.
- [4] I. Fidan *et al.*, “Recent Inventions in Additive Manufacturing: Holistic Review,” *Inventions 2023, Vol. 8, Page 103*, vol. 8, no. 4, p. 103, Aug. 2023, doi: 10.3390/INVENTIONS8040103.
- [5] T. Ingrassia, V. Nigrelli, V. Ricotta, and C. Tartamella, “Process parameters influence in additive manufacturing,” *Lecture Notes in Mechanical Engineering*, vol. 0, pp. 261–270, 2017, doi: 10.1007/978-3-319-45781-9\_27/COVER.
- [6] K. Anwar, M. Said, M. Afizal, and M. Amin, “Overview on the Response Surface Methodology (RSM) in Extraction Processes,” *Journal of Applied Science & Process Engineering*, vol. 2, no. 1, pp. 8–17, Apr. 2015, doi: 10.33736/JASPE.161.2015.
- [7] P. Biswas, S. Mamatha, S. Naskar, Y. S. Rao, R. Johnson, and G. Padmanabham, “3D extrusion printing of magnesium aluminate spinel ceramic parts using thermally induced gelation of methyl cellulose,” *J Alloys Compd*, vol. 770, 2019, doi: 10.1016/j.jallcom.2018.08.152.
- [8] L. Ren *et al.*, “Process parameter optimization of extrusion-based 3D metal printing utilizing PW-LDPE-SA binder system,” *Materials*, vol. 10, no. 3, 2017, doi: 10.3390/ma10030305.
- [9] Y. Thompson, J. Gonzalez-Gutierrez, C. Kukla, and P. Felfer, “Fused filament fabrication, debinding and sintering as a low cost additive manufacturing method of 316L stainless steel,” *Addit Manuf*, vol. 30, 2019, doi: 10.1016/j.addma.2019.100861.
- [10] C. Tosto, J. Tirillò, F. Sarasini, C. Sergi, and G. Cicala, “Fused deposition modeling parameter optimization for cost-effective metal Part Printing,” *Polymers (Basel)*, vol. 14, no. 16, Aug. 2022.
- [11] Z. Zhang, J. Femi-Oyetero, I. Fidan, M. Ismail, and M. Allen, “Prediction of dimensional changes of low-cost metal material extrusion fabricated parts using machine learning techniques,” *Metals (Basel)*, vol. 11, no. 5, 2021, doi: 10.3390/met11050690.
- [12] M. Norris, I. Fidan, and M. Allen, “Rheological Characterization of Room Temperature Powder Metal Paste for Extruded Material Modeling,” in *International Solid Freeform Fabrication Symposium*, Austin, TX, 2022.
- [13] S. A. Weissman and N. G. Anderson, “Design of Experiments (DoE) and Process Optimization. A Review of Recent Publications,” *Org Process Res Dev*, vol. 19, no. 11, pp. 1605–1633, Nov. 2015, doi: 10.1021/OP500169M/ASSET/IMAGES/LARGE/OP-2014-00169M\_0027.JPEG.
- [14] M. Alshaiikh Ali, I. Fidan, M. Allen, I. Bhattacharya, and K. Tantawi, “Utilizing Lattice Infill Structures to Optimize Weight with Structural Integrity Investigation for Commonly Used 3D Printing Technologies,” in *Proceedings of the SFF2022-33rd Annual*



- International Solid Freeform Fabrication Symposium-An Additive Manufacturing Conference*, Austin, TX, Jul. 2022.
- [15] E. R. Fitzharris, I. Watt, D. W. Rosen, and M. L. Shofner, “Interlayer bonding improvement of material extrusion parts with polyphenylene sulfide using the Taguchi method,” *Addit Manuf*, vol. 24, pp. 287–297, Dec. 2018, doi: 10.1016/J.ADDMA.2018.10.003.
- [16] J. B. Schamburg and D. E. Brown, “A generalized multiple response surface methodology for complex computer simulation applications,” in *Proceedings - Winter Simulation Conference*, 2004. doi: 10.1109/wsc.2004.1371414.
- [17] G. Singh, J. M. Missiaen, D. Bouvard, and J. M. Chaix, “Copper extrusion 3D printing using metal injection moulding feedstock: Analysis of process parameters for green density and surface roughness optimization,” *Addit Manuf*, vol. 38, 2021, doi: 10.1016/j.addma.2020.101778.
- [18] M. A. Ali, I. Fidan, and K. Tantawi, “Investigation of the impact of power consumption, surface roughness, and part complexity in stereolithography and fused filament fabrication,” *International Journal of Advanced Manufacturing Technology*, 2023, doi: 10.1007/s00170-023-11279-3.
- [19] Z. Zhang and I. Fidan, “Machine Learning-Based Void Percentage Analysis of Components Fabricated with the Low-Cost Metal Material Extrusion Process,” *Materials*, vol. 15, no. 12, 2022, doi: 10.3390/ma15124292.